Optical Design and Requirements for the Normal Incidence X-ray Telescope of the Reconnection and Microscale Solar Probe

Paul B. Reid[+a], Paul Glenn[b], and Jay Bookbinder[a]
[a]Harvard-Smithsonian Center for Astrophysics, 60 Garden St., Cambridge MA USA 02138
[b]Bauer Associates, 8 Tech Circle, Natick MA USA 01760

ABSTRACT

One of the key instruments on the Reconnection and Microscale (RAM) Solar-Terrestrial Probe mission is a normal incidence multilayer x-ray telescope designed to provide 10 milli-arc-sec imaging of the solar corona. To achieve this level of imaging it will be necessary to fabricate meter-class reflective optics with diffraction limited performance at 193 Angstroms. Because of the use of multilayer optics, surface micro-roughness must also be maintained at very low levels (a few Angstroms rms) to maintain good reflectance.

To ease fabrication constraints and the sometimes competing requirements of micro-roughness and figure, we have explored a number of potential designs and fabrication approaches for RAM. Figure error budgets and optical designs are shown, demonstrating that RAM can be built with existing mirror fabrication technology.

Keywords: x-ray optics, normal incidence optics, EUV imaging, Sun, corona

1. INTRODUCTION

The Recombination and Microscale mission is a Solar-Terrestrial Probe class mission designed to explore the Sun's outer atmosphere at the highest possible spatial, spectral, and temporal resolution[1]. Proposed in 1998 by the Harvard-Smithsonian Center for Astrophysics was an ultra-high resolution EUV telescope with the goal of examining the basic small-scale processes in hot magnetized plasmas that are common throughout the Universe. Originally envisioned as the NASA MIDEX (medium sized explorer) mission HIREX, the mission has evolved to the Solar-Terrestrial Probe Mission RAM. In 2000, the NASA Sun-Earth Connection (SEC) Roadmap Committee selected the RAM S-T probe as a long term mission. The mission continues to be in the SEC Roadmap with a planned launch in the 2014 timeframe. Additional discussion of RAM science can be found in Golub *et. al.*[2].

Because of the desire for diffraction limited performance at EUV wavelengths, mirror figure requirements are extremely tight, resulting in more difficult mirror fabrication. In an effort to ease fabrication requirements, we examine a range of optical designs within the framework of finding whether one design appears significantly easier (and therefore also less expensive) to produce.

2. RAM NORMAL INCIDENCE HIGH RESOLUTION TELESCOPE

RAM will carry five instruments to address a broad range of solar physics phenomena: the High Resolution Imager (HRI) whose optics are discussed in this paper, the X-ray Calorimeter (XRC), an EUV Spectrometer (EUVSPEC), an Intermediate Scale Imager (ISI), and a Hard X-ray Camera (HRC). These instruments are discussed in references (1) and (2).

The HRI will provide system resolution of 0.02 arc-sec (~ 14 km on the Sun) over an approximate 2.5 arc-min (diameter) field-of-view, over a narrow wavelength bandwidth centered at 193 Angstroms. This bandwidth enables Fe XXIV emission, covering a temperature range of ~ 1 million to 15 million degrees Kelvin. Overall telescope design is

[+] preid@cfa.harvard.edu; phone 1 617 495-7233; fax 1 617 495-7356

Optics for EUV, X-Ray, and Gamma-Ray Astronomy II, edited by Oberto Citterio, Stephen L. O'Dell,
Proc. of SPIE Vol. 5900, 59000K, (2005) · 0277-786X/05/$15 · doi: 10.1117/12.613951

measurement of Fe XII and an ~ 0.6 m diameter off-axis Cassegrain with an ~ 250 m effective focal length (EFL). The off-axis design enables us to employ an unobscured aperture, minimizing diffraction. With 12 μm sized pixels, the long EFL results in an ~ 0.01 arc-sec /pixel plate scale. The two mirrors are separated by an ~ 30 m long extendible optical bench (EOB), with a 6-axis controlled secondary mirror for on-orbit alignment and an active image stabilization (tip/tilt) system. More detailed discussion of the EOB, on-orbit alignment, image stabilization system, and mirror mounting technology is found in reference (1).

3. OPTICS DESIGN TRADES

We examined three different classes of optical designs. In the first both primary and secondary mirrors are aspheric. This type of design offers the promise of the best performance over the largest field of view (FOV). As a trade, however, both optics must be precisely figured and smoothed to maintain imaging, scatter, and reflectance performance. In combination with achieving aspheric figure this may be a more difficult fabrication task. The second design entails an aspheric primary mirror and a spherical secondary, thereby easing somewhat fabrication difficulties. Lastly, we considered the case of a spherical primary and an aspheric secondary mirror. Given the size of the primary mirror (600 mm diameter) and estimated aspheric departure, this option likely represents the least challenging optical fabrication option.

Mirror prescriptions were optimized over three different field sizes for each of the three designs: 0.625, 1.25, and 2.5 arc-min radius FOVs. The figure of merit we used was average root mean square (RMS) wavefront error [averaged over the field]. Anamorphic aspheres were used wherein the aspheric surface is represented as:

$$s(\rho,\theta) = \frac{c \cdot \rho^2}{1+\sqrt{1-c^2\rho^2}} + \sum_{1}^{11} a_i \cdot Z_i(\rho,\theta) \qquad (1),$$

where ρ and θ are the polar coordinates, c is the curvature equal to the inverse of the radius of curvature, Z_i are the standard set of circular Zernike polynomials, and a_i are the polynomial coefficients. Z_{11}, the highest order Zernike employed in the optimization, corresponds to 3rd order spherical aberration. Thus the aspheric surfaces were represented as spheres plus some set of Zernike polynomials including 3rd order astigmatism, coma, and spherical aberration. The optical raytracing software package ZEMAX™ was used. Parameters employed in the raytracing are listed in Table 1.

In figure 1 we plot the field averaged RMS wave front error for the three designs for each of the three FOV cases. We observe that the double asphere design clearly produces the lowest RMS residual wavefront error of the three designs, well below the Marechal criterion for diffraction limited performance (defined as a Strehl ratio of 0.80, equal to a wavefront error of 0.0752λ, RMS)[3]. Second, we clearly see that the spherical primary/aspheric secondary design does not achieve diffraction limited performance averaged over any of the fields we specified. Lastly, we see that the aspheric primary/spherical secondary meets or surpasses the diffraction limited performance criteria for fields of view of 0.625 and 1.25 arc-min radius. Because the spherical primary design does not achieve diffraction limited performance, we eliminate it from further trade comparisons.

In figures 2 and 3 we show the encircled energy for the double asphere and spherical secondary designs. In both cases perfect optics (zero figure error and misalignment) are assumed. Encircled energy curves are for a number of field positions. We observe that within the +/- 1.25 arc-min field (+/- 0.0208 deg) performance between the two designs is relatively indistinguishable, and both cases come close to matching the theoretical limit of aperture diffraction. Beyond the +/- 1.25 arc-min field the spherical secondary design starts to significantly underperform relative to the diffraction limit.

Primary mirror	
Diameter:	600 mm
Radius of curvature (concave):	60.75 m
Form:	two versions: * sphere * anamorphic asphere (much less than one wave of asphericity at 6328 Angstroms)
Secondary mirror	
Diameter:	77 mm (for +/- 0.625 arc-minute field) 86 mm (for +/- 1.25 arc-minute field) 106 mm (for +/- 2.5 arc-minute field)
Radius of curvature (convex):	7.69 m
Form:	two versions: * sphere * anamorphic asphere (much less than one wave of asphericity at 6328 Angstroms)
Primary-secondary separation:	27.00 m
Plate scale:	1.20 mm / arc-second (or, 12.0 microns per 0.01 arc-second)
Effective focal length:	248 m
Central wavelength:	193 Angstroms
Field of view	* +/- 0.625 arc-minutes * +/- 1.25 arc-minutes * +/- 2.5 arc-minutes

Table 1. – Optical design parameters.

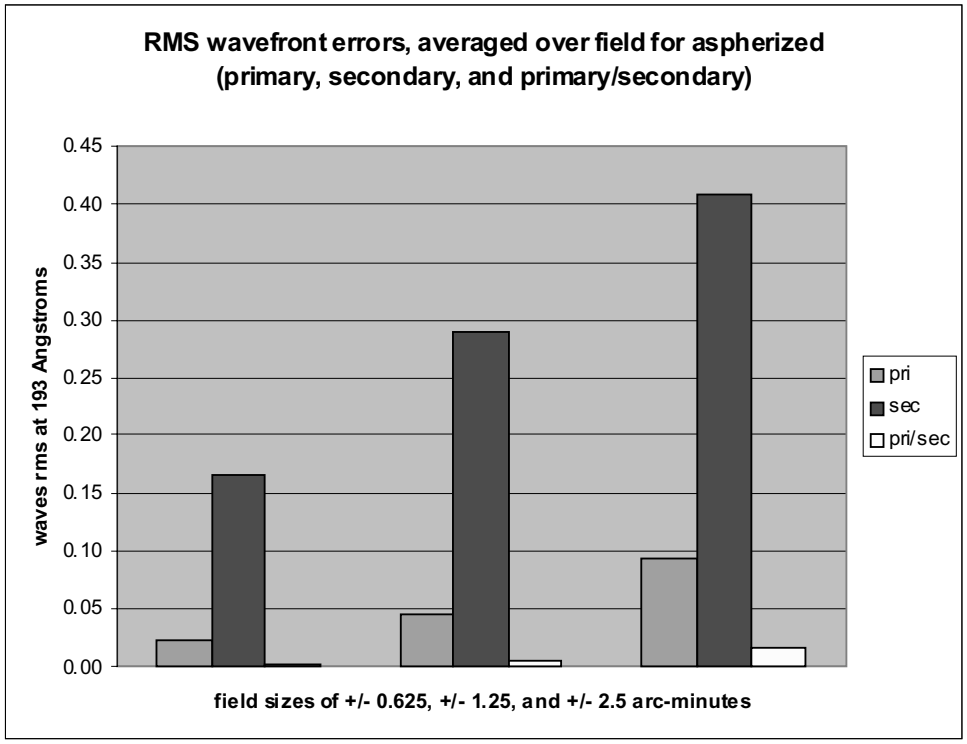

Figure 1. - RMS residual wavefront errors (i.e., those inherent in the optical design) as a function of field of view, and whether the asphericity is allowed on the primary, secondary, or both.

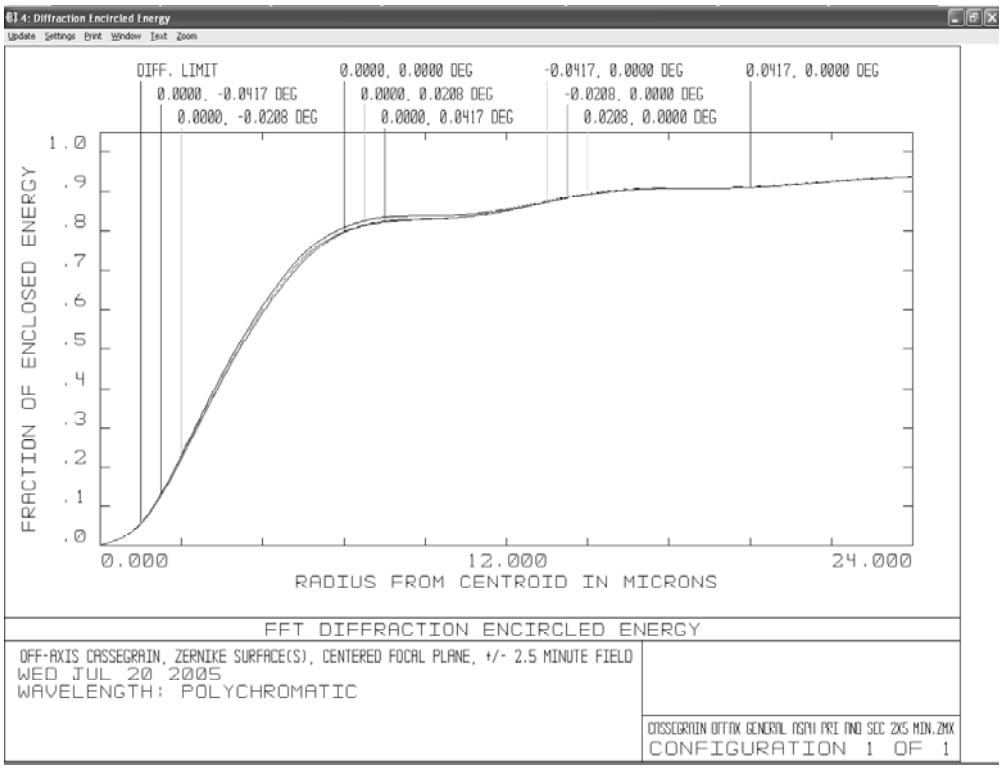

Figure 2.- Encircled energy for the two asphere design. The wavelength is 193 nm.

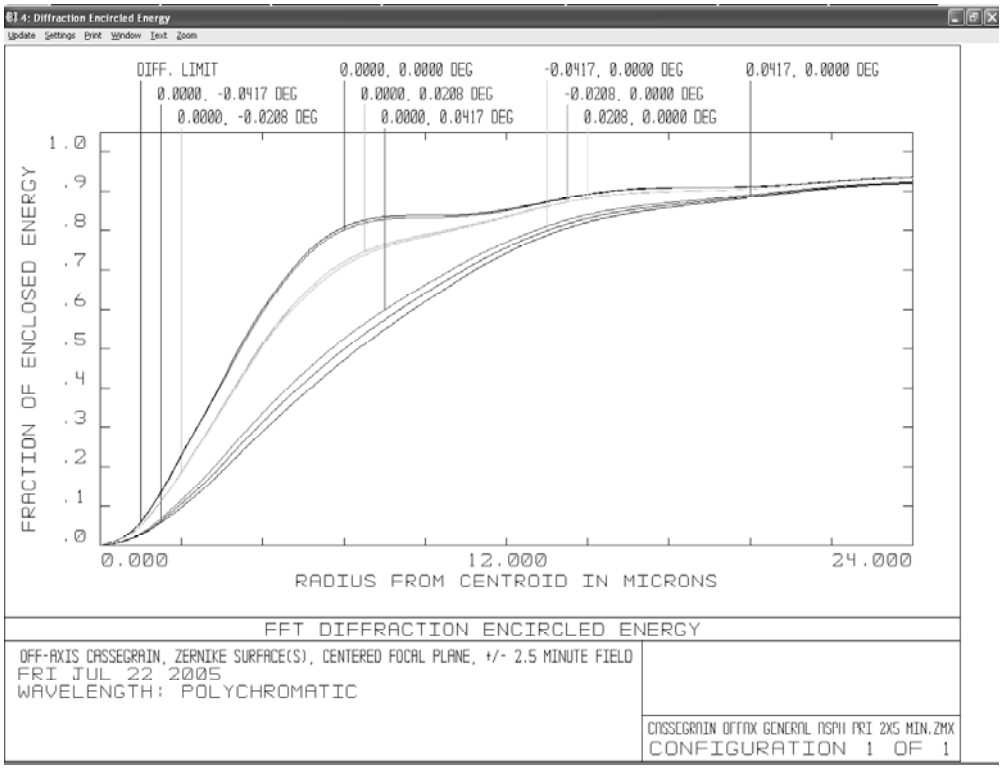

Figure 3.- Encircled energy for the spherical secondary mirror design. Again, the wavelength is 193 nm.

In figures 4-6 we show the aspheric departure for the primary and secondary in the two asphere design (figures 4, 5) and the primary in the spherical secondary design (figure 6). We note that the rms amplitude of the aspheric departures is 16.2 nm for the primary and 2.6 nm for the secondary in the two asphere system, and 16.0 nm for the primary in the spherical secondary system. These values, plus the shapes in figures 4 and 6, reveal that there is very little figure difference between the two primaries.

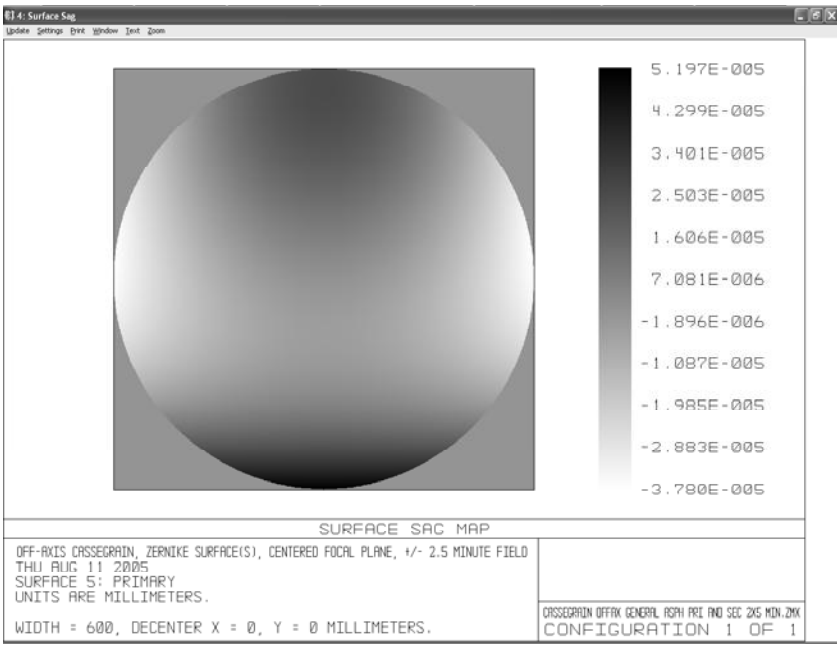

Figure 4.- Aspheric departure of primary mirror in dual asphere design.

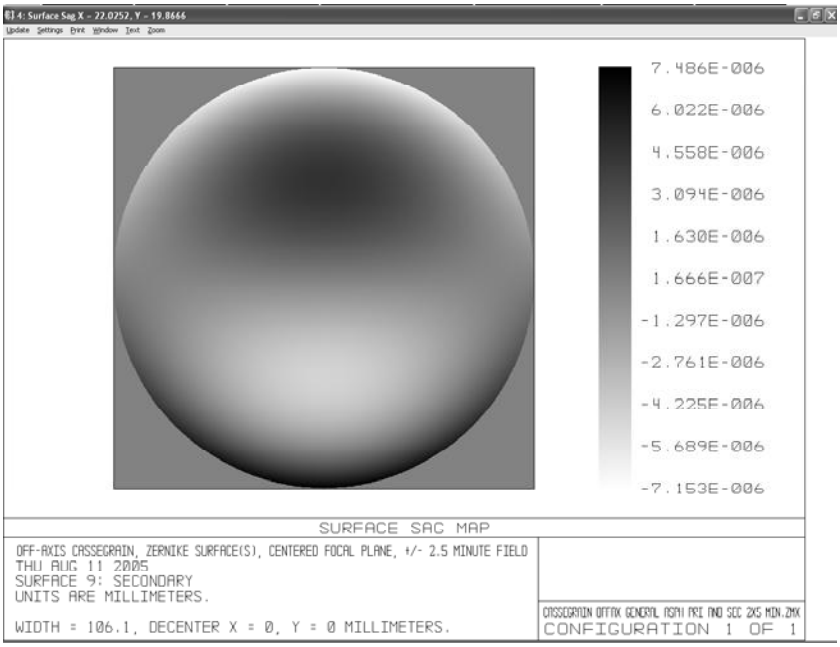

Figure 5.- Aspheric departure of secondary mirror in the dual asphere design. This mirror is sized for a 2.5 arc-min (radius) field of view.

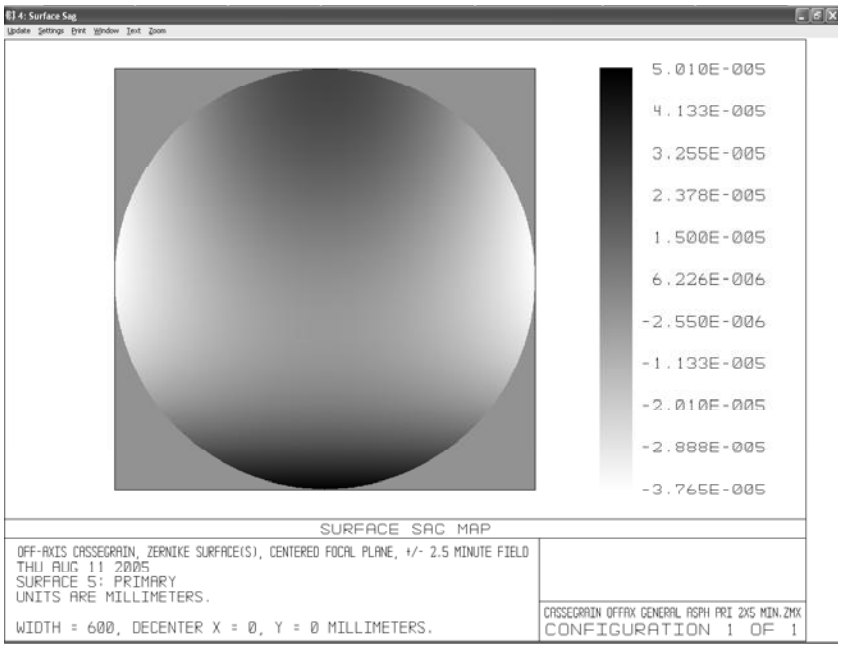

Figure 6.- Aspheric departure of primary mirror in spherical secondary design.

4. OPTICS REQUIREMENTS

Once the optic prescriptions are determined we need to estimate optic requirements for the two successful designs. We divide figure error spatial frequencies into 3 bandwidths; figure error, roughness, and micro-roughness.

Figure error covers the lowest bandwidth. Diffraction limited resolution, as represented by the Rayleigh criterion, is 0.008 arc-sec, radius. With a 0.01 arc-sec radius resolution requirement for the optics, essentially all spatial frequency errors, expressed as an integer number of cycles/aperture, degrade performance and are treated with a physical optics model. We define figure error as those errors giving rise to small angle scatter, thereby degrading imaging. We use a bandwidth for figure error of 1 to 120 cycles/aperture. This is equivalent to ~ 0.00167 to 0.2 mm^{-1} for the primary mirror and ~ 0.013 to 1.5 mm^{-1} for the secondary. We set the upper bandwidth limit somewhat arbitrarily from the standpoint of what might be reasonable for a single metrology instrument. For example, setting the upper limit at 100 cycles/aperture is a nice round number, but the corresponding 6 mm spatial error period could prove difficult for some higher bandwidth instruments that might be used to measure roughness, the next higher bandwidth group of errors. Note also that the 120 cycles/aperture also roughly corresponds to a scatter angle of 1 arc-second.

We estimate the allowable figure error by requiring an encircled energy fraction of 0.68 within a 0.01 arc-sec radius. This is equivalent to saying we require 1 – *Total Integrated Scatter* = 0.68 , where the *Total Integrated Scatter TIS* is given by the Strehl formula:

$$Strehl = \exp -\left(k \cdot \sigma\right)^2 \qquad (2),$$

where $k = 2\pi/\lambda$, and σ is the system wavefront error. If we let σ be composed of the design residual wavefront error and the mirror figure wavefront error (twice the surface error), than the total *Strehl* is just the product of the two contributing *Strehl*s. Review of figures 2 and 3 reveal that the 0.01 arc-sec radius fractional encircled energy is ~ 0.83 for the two asphere design and ~ 0.81 for the spherical secondary design. These represent the design residual *Strehl* factor. Multiplicatively, these require the mirror figure *Strehl*s to be 0.82 and 0.84 for the two and single asphere designs,

respectively. Eq. (2) can be solved for σ. This resulting value for the total mirror wavefront error is then divided by two to get two element surface error, and then apportioned between the primary and secondary mirrors assuming all the wavefront errors are uncorrelated. In this manner we arrive at an allocation of 6.84 A, RMS, for the combined surface errors in the two asphere system, and an allocation of 6.41 A, RMS, for the combined surface in the spherical secondary system. We somewhat arbitrarily apportion these errors between the primary and secondary mirrors as shown in Table 2, although the more important point is the root sum square of the two rms surface figures.

We define roughness errors as those which scatter outside the figure errors, but still scatter within the field of view. We use a frequency bandwidth of 0.2 to 20 mm^{-1} for the primary mirror and 1.5 to 150 mm^{-1} for the secondary mirror, corresponding to ~ 1 to 100 arc-sec scatter angle. This range of scatter primarily affects image contrast. We require the two surface Strehl factor due to roughness errors to be 0.9. This corresponds to a two surface RMS error of ~ 5 A, or 3.5 A, RMS, per surface.

Design Case	RMS Figure Amplitude (in Angstroms, surface)		
	Total (two surfaces)	Primary Mirror	Secondary Mirror
Two aspheric surfaces	6.84	5.3	4.3
Spherical secondary	6.41	5	4

Table 2.- Mirror figure requirements for the two different designs.

Lastly, we define micro-roughness (in the manner of Windt[4]) as those errors which scatter outside the detector and so essentially reduce effective area. Thus this bandwidth runs from 20 to 52,000 mm^{-1} for the primary mirror and 150 to ~ 52,000 mm^{-1} for the secondary mirror. Again applying the Strehl factor here we limit the micro-roughness to 5 A, RMS, per surface. This corresponds to an approximate 20 per cent reduction in effective area (reflectance). Note that while this rms amplitude is much larger than typically specified for multilayer coated optic micro-roughness, it actually encompasses much lower spatial frequencies than typically considered. The inclusion of these lower frequencies will effectively drive the rms amplitude, resulting in relatively smooth surfaces in the AFM (atomic force microscope) spatial frequency bandwidth as is more typical with soft x-ray normal incidence mirrors.

Roughness and micro-roughness surface error requirements are summarized in Table 3.

Parameter	RMS Amplitudes (in Angstroms, surface)		
	Total (two surfaces)	Primary Mirror	Secondary Mirror
Roughness	5	3.5	3.5
Micro-roughness	7	5	5

Table 3 – Roughness and micro-roughness requirements.

We can compare the mirror requirements with optics developed for extreme ultraviolet lithography (EUVL), operating at a wavelength of 134 A. Recent results[5] have shown aspheric surface figure of ~ 2.7 A, RMS, has been achieved on optics of ~ 400 mm size. In addition, Goldberg et. al.[5] have also demonstrated figure metrology accuracy of 1 A, RMS. We see that little extension of developing EUVL capabilities is required for RAM HRI optics fabrication.

5. SUMMARY

We have examined three different Cassegrain telescope designs for the normal incidence high resolution imaging telescope of the Reconnection and Microscale Probe. The purpose of this examination was to determine whether there is a significant fabrication advantage of one design relative to another, while still meeting performance requirements. We find excellent performance is achieved with the largest field of view when a two asphere design is employed. A single

asphere design utilizing a spherical secondary mirror also meets performance requirements although it requires slightly better mirror figure than the two asphere design, and also cannot achieve as large a field of view and still meet requirements. The third design, another single asphere one with a spherical primary mirror, does not meet telescope requirements. We also note that while a spherical secondary mirror can be used to meet requirements, the magnitude of the aspherization is quite small (~2.6 nm, RMS). Depending upon the fabrication process, this amplitude aspherization may not have any adverse impact upon fabrication. In that case, the two asphere design offers significant advantages over the spherical secondary design with respect to field of view, and small advantages with respect to mirror figure.

We have also estimated mirror figure, roughness, and micro-roughness requirements. While extremely challenging, the requirements for these optics are not inconsistent with requirements and achievements in extreme ultraviolet lithography.

6. REFERENCES

1. Bookbinder, J., *et. al.*, "The Reconnection And Microscale (RAM) Solar-Terrestrial Probe", SPIE Proc. vol. **4853**, 436 (2003).

2. Golub, L., *et. al.*, "The reconnection and microscale (RAM) probe," SPIE Proc. vol. **5901**, *to be published*.

3. Smith, Warren J., "Modern Optical Engineering," (McGraw-Hill, New York), 3rd ed., p. 357, 2000.

4. Windt, D.L., Waskiewicz, W.K., and Griffith, J.E., "Surface finish requirements for soft x-ray mirrors," Appl. Opt. 33, No. 10, 2025 (1994).

5. Goldberg, K.A., "Ultra-high accuracy optical testing: creating diffraction-limited short-wavelength optical systems,", SPIE Proc., *this proceedings volume*.